Effect of roughness on interface shear behavior of sand with steel and concrete surface

Manojit Samanta[*1], Piyush Punetha[2a] and Mahesh Sharma[2b]

[1]*Geotechnical Engineering Group, CSIR-Central Building Research Institute, Roorkee–247667, Uttarakhand, India*
[2]*Academy of Scientific and Innovative Research, CSIR-Central Building Research Institute, Roorkee 247667, Uttarakhand, India*

Abstract.   The present study evaluates the interface shear strength between sand and different construction materials, namely steel and concrete, using direct shear test apparatus. The influence of surface roughness, mean size of sand particles, relative density of sand and size of the direct shear box on the interface shear behavior of sand with steel and concrete has been investigated. Test results show that the surface roughness of the construction materials significantly influences the interface shear strength. The peak and residual interface friction angles increase rapidly up to a particular value of surface roughness (critical surface roughness), beyond which the effect becomes negligible. At critical surface roughness, the peak and residual friction angles of the interfaces are 85-92% of the peak and residual internal friction angles of the sand. The particle size of sand (for morphologically identical sands) significantly influences the value of critical surface roughness. For the different roughness considered in the present study, both the peak and residual interaction coefficients lie in the range of 0.3-1. Moreover, the peak and residual interaction coefficients for all the interfaces considered are nearly identical, irrespective of the size of the direct shear box. The constitutive modeling of different interfaces followed the experimental investigation and it successfully predicted the pre-peak, peak and post peak interface shear response with reasonable accuracy. Moreover, the predicted stress-displacement relationship of different interfaces is in good agreement with the experimental results. The findings of the present study may also be applicable to other non-yielding interfaces having a similar range of roughness and sand properties.

Keywords: interface; surface roughness; direct shear test; peak interface angle; residual interface angle; constitutive modeling

1. Introduction

Frictional strength at the interface between soil and other construction materials is a critical parameter for the design of a wide range of geotechnical structures. Estimation of a reliable interface frictional strength is inevitable to accurately predict the vertical load carrying capacity of piles, pull out capacity of soil reinforcements, design of retaining walls etc. (Aksoy *et al.* 2016, Sharma *et al.* 2016, 2017). The interface shear strength properties should be accounted for, in the design and must be computed with fair accuracy for safe design.

The soil-construction material interface shearing mechanism highly depends on the surface roughness of the construction material in contact with the soil. Only friction is predominant for surfaces with a low surface roughness while interlocking and mobilization of passive resistance are predominant for surfaces with high surface roughness. Thus, friction and interlocking accompanied by passive

resistance are the two governing mechanisms for the mobilization of interface shearing resistance of construction material with soil.

A large number of researchers have studied the effect of different parameters on the interface shear behavior of soil with different materials through direct shear tests (Potyondy 1961, Butterfield and Andrawes 1972, Acar *et al.* 1982, Tsubakihara and Kishida 1993, Tejchman and Wu 1995, Reddy *et al.* 2000, Gireesha and Muthukkumaran 2011, Vieira *et al.* 2015, Cabalar 2016, Zhang *et al.* 2016, Punetha *et al.* 2016, 2017, Punetha and Samanta 2017, Toufigh *et al.* 2017). The size of direct shear box affects the response of the soil-construction material interface to a large extent. Cerato and Lutenegger (2006) tested five types of sand at different relative density in three square shear boxes of varying sizes (60 mm, 101.6 mm and 304.8 mm). They concluded that the friction angle decreases with an increase in box size but increases with an increase in the relative density of sand for each size of the box. Yoshimi and Kishida (1981) investigated the interface frictional strength between steel and three different sands using the ring torsional shear apparatus. Results showed that the interface friction is dependent on the surface roughness of the materials. The residual angle of interface friction was found to be independent of normal stress and the type of sand. Despite a significant number of studies on the soil-material interface, a very few of them deal with the effect of surface roughness and mean particle size of sands having identical

---

∗Corresponding author, Scientist
 E-mail: manojit_samanta@rediffmail.com
[a]Research Scholar
 E-mail: punetha.piyush@yahoo.in
[b]Trainee Scientist
 E-mail: mahesh3.ce@gmail.com

morphological characteristics, on the interface shear strength. Moreover, the morphological parameters of the particles and surface roughness have been quantified in a limited number of studies which makes it difficult to apply and compare their findings. Limited literature is available regarding the effect of surface roughness on the residual interface friction angle.

Several constitutive models have been developed to describe the interface behavior between granular soil and metal. These models predict the linear or non-linear elastic stress-displacement relationship of the interfaces (Duncan and Clough 1971, Goodman *et al.* 1968, Desai *et al.* 1984). Some advanced constitutive models are also able to capture the elastoplastic, strain hardening/softening, cyclic loading behavior of the interfaces (Boulon and Nova 1990, Desai and Ma 1992, Shahrour and Rezaie 1997, Aubry *et al.* 1990, De Gennaro and Frank 2002, Liu *et al.* 2006).

The present study investigates the interface shear strength parameters of steel and concrete surface having different roughness, with sand in the direct shear test. Two poorly graded sand samples with different mean particle size but identical morphological characteristics (angularity, sphericity and roundness) have been taken to nullify the effect of morphology on the frictional properties. The influence of relative density of sand and size of the direct shear box on the interface shear behavior have also been investigated. Further, two different constitutive models have been used to predict the observed stress–displacement relationship of different interfaces involving sand and steel/concrete. The paper is presented in the following sequence, first a quantitative effect of different parameters on the interface shear strength is presented. Then, the constitutive models are used to predict the stress-displacement relationship of the different interfaces.

2. Materials

2.1 Sand

Two types of river sand are used in the present study which were collected from the nearby site of the CBRI campus. Grain size distribution curve of the two river sands is presented in Fig. 1. Other relevant geotechnical properties are presented in Table 1. Both the soil samples are classified as poorly graded sand (SP) as per Indian Standard. Mean grain size (D_{50}) of the sand 1 and sand 2 (referred as S1 and S2 henceforth) are 1.2 mm and 0.23 mm respectively. The morphological characteristics of the sand particles have been evaluated using digital image processing. Figs. 2(a) and 2(c) show the microscopic images of the sand particles S1 and S2 respectively. Figs. 2(b) and 2(d) show the procedure used to determine the morphological parameters. Image of the particles along with the equivalent ellipse, having the same area and aspect ratio is depicted in the figures. The perimeter and area of the sand particle and the corresponding equivalent ellipse are used to calculate the angularity, sphericity and roundness of the particle. About 50 particles were taken for the morphological analysis (Vangla and Latha 2016). Table 2 shows the average values
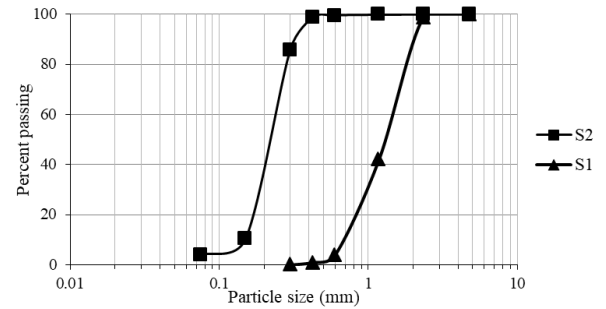

Fig. 1 Grain size distribution of sand

Table 1 Properties of sand medium

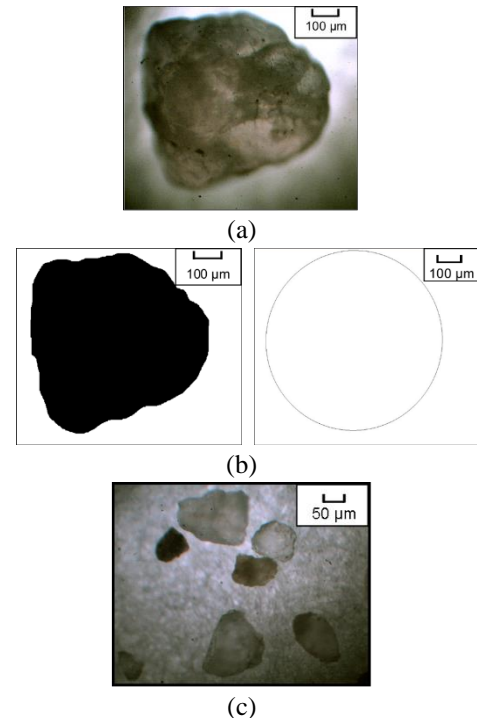| Properties	Sand 1 (S1)	Sand 2 (S2)
Sand (%)	100	98
Silt (%)	0	2
Clay (%)	0	0
D_{10}	0.7	0.11
D_{30}	0.95	0.17
D_{50}	1.2	0.23
Coefficient of uniformity (C_u)	2.29	1.92
Coefficient of curvature (C_c)	0.8	1.15
Specific gravity (G)	2.65	2.67
Minimum dry unit weight (kN/m^3)	14.67	13.90
Maximum dry unit weight (kN/m^3)	15.87	16.60
IS classification	SP	SP

Fig. 2 Morphological analysis of sand: (a) image of sand particle (S1) taken using optical microscope, (b) sand particle (S1) and its equivalent ellipse to determine morphological characteristics, (c) image of sand particles (S2) taken using optical microscope and (d) sand particles (S2) and their equivalent ellipse to determine morphological characteristics
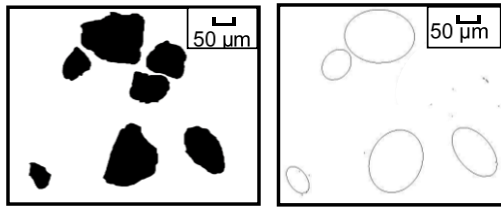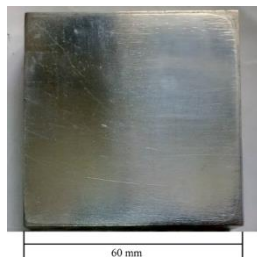
(d)

Fig. 2 Continued

Table 2 Morphological characteristics of sand

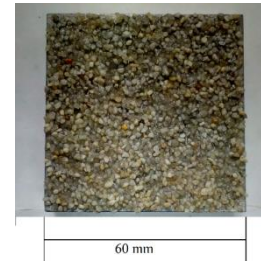| Parameters	Sand 1 (S1)	Sand 2 (S2)
Angularity	1.13	1.15
Sphericity	0.91	0.93
Roundness	0.71	0.76

(a)

(b)

(c)

(d)

Fig. 3 Different interface materials used in the present study, (a) well finished mild steel surface (MS1), (b) mild steel surface with scratches (MS2), (c) fine sand glued mild steel surface (MSF), (d) concrete (C) and (e) coarse sand glued mild steel surface (MSC)
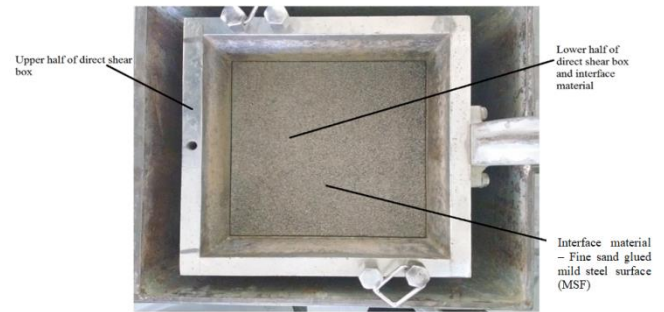

(e)

Fig. 3 Continued

Fig. 4 Direct shear box with interface material

of the different parameters (angularity, sphericity and roundness) for both sand samples. It is clear that both the sand samples possess identical morphological characteristics and can be classified as sub rounded.

2.2 Structural material

Steel and concrete are the most commonly used structural materials in the field of geotechnical engineering. Both find application in the construction of shallow and deep foundations, retaining structures and sheet pile walls etc. Therefore, steel and concrete surfaces are considered for the present interface study. Four different types of mild steel surfaces with different surface roughness and one concrete surface have been used to investigate the effect of surface roughness on the interface behavior. Different degree of surface roughness on the mild steel surface is generated by gluing sand particles of different sizes. The concrete interface is prepared in a specially fabricated mold having the same dimension as the lower half of the direct shear box. Fig. 3 shows the different interfaces used in the present investigation. Well finished mild steel surface, mild steel surface with scratches, fine sand glued mild steel surface, concrete surface, coarse sand glued mild steel surface are referred as MS1, MS2, MSF, C and MSC respectively for reference purpose. Special care has been taken to ensure that the sand particles glued on the steel surfaces remain intact. After each test, roughness parameters of the sand glued interfaces are measured to check the variability of roughness before and after the tests. Results of the interface tests were discarded if the variation in surface roughness of the interface was more than 5% before and after the test. The size of the interface material is selected such that it perfectly fits into the lower half of the direct shear box and allows shearing of the sand at its face. Fig. 4 shows the direct shear box along with structural interface material in the lower half of the box.

Table 3 Surface roughness of different interfaces with S1

Surface type	R_{max} (mm)	Normalized roughness, S1 ($R_n = R_{max}/D_{50}$) $\times 10^{-3}$	Normalized roughness, S1 ($R_n = R_a/$Wt. Avg.) $\times 10^{-3}$	Normalized roughness, S1 ($R_n = R_{max}/$Wt. Avg.) $\times 10^{-3}$	Normalized roughness, S1 ($R_n = R_a/D_{50}$) $\times 10^{-3}$
MS1	0.001	0.83	0.58	0.59	0.81
MS2	0.05	42	27	29	38
C	0.29	242	56	171	80
MSF	0.44	367	65	259	92
MSC	0.62	517	125	365	177

Table 4 Surface roughness of different interfaces with S2

Surface type	R_{max} (mm)	Normalized roughness, S2 ($R_n = R_{max}/D_{50}$) $\times 10^{-3}$	Normalized roughness, S2 ($R_n = R_a/$Wt. Avg.) $\times 10^{-3}$	Normalized roughness, S2 ($R_n = R_{max}/$Wt. Avg.) $\times 10^{-3}$	Normalized roughness, S2 ($R_n = R_a/D_{50}$) $\times 10^{-3}$
MS1	0.001	4.35	3.6	3.70	4.2
MS2	0.05	217	169	185	199
C	0.29	1261	353	1074	415
MSF	0.44	1913	410	1630	482
MSC	0.62	2696	790	2296	927

3. Roughness of the interface materials

The surface roughness of each interface material was measured using a surface profilometer. Roughness measurement was taken at five different profile segments along the longitudinal and transverse direction to characterize the surface and check the uniformity in roughness values (Dove and Jarrett 2002). Kishida and Uesugi (1987) expressed roughness as the ratio of relative height between the highest peak and the lowest trough of surface profile (R_{max}) to the mean particle size (D_{50}) of soil, over a length equal to the mean particle size of soil. Whereas, Subba Rao *et al.* (1998) expressed the interface roughness as the ratio of the average value of roughness (R_a) to the weighted average (Wt. Avg.) of the different fraction of soil particles. Tables 3 and 4 show the normalized roughness (R_n) values obtained for different type of interfaces from the above two approaches for sand S1 and S2 respectively. The roughness of the interfaces in the present study is quantified and expressed in terms of R_{max}, R_a and R_n. The roughness values are also expressed in the form of R_{max}/Wt. Avg. and R_a/D_{50} for all the interfaces. It must be noted that the traverse length in the present study has been taken as 50 mm instead of a length equal to the mean particle size, as specified in the other studies. This is done to acquire sufficient information for the accurate estimation of roughness parameters. Well finished mild steel surface has the least surface roughness ($R_{max}=1$ μm), while the S1 sand glued interface has the maximum surface roughness ($R_{max}=620$ μm). According to FHWA (2003) design guidelines, the maximum surface roughness values for steel, FRP composite and finished concrete surfaces are 30 μm, 40 μm and 220 μm respectively. Moreover, Frost *et al.* (2002) studied the shear failure behavior of sand and structural material interfaces having roughness (R_{max}) in the range of 5-500 μm. Therefore, the results of the present study may also be applicable to other non-yielding interfaces as specified above with a similar range of

roughness and sand medium properties.

4. Experimental procedure

In the present study, most of the interface direct shear tests have been performed on the direct shear box of size 60 mm×60 mm×25 mm at 80% relative density (RD). A few tests have also been conducted on a direct shear box of size 300 mm×300 mm×125 mm to investigate the effect of box size on the interface shear strength. Interface materials were placed on the lower half of the direct shear box. Special care was taken to ensure that the top face of interface and top of the lower half of direct shear box were at the same level. The upper half of the box was filled with the required
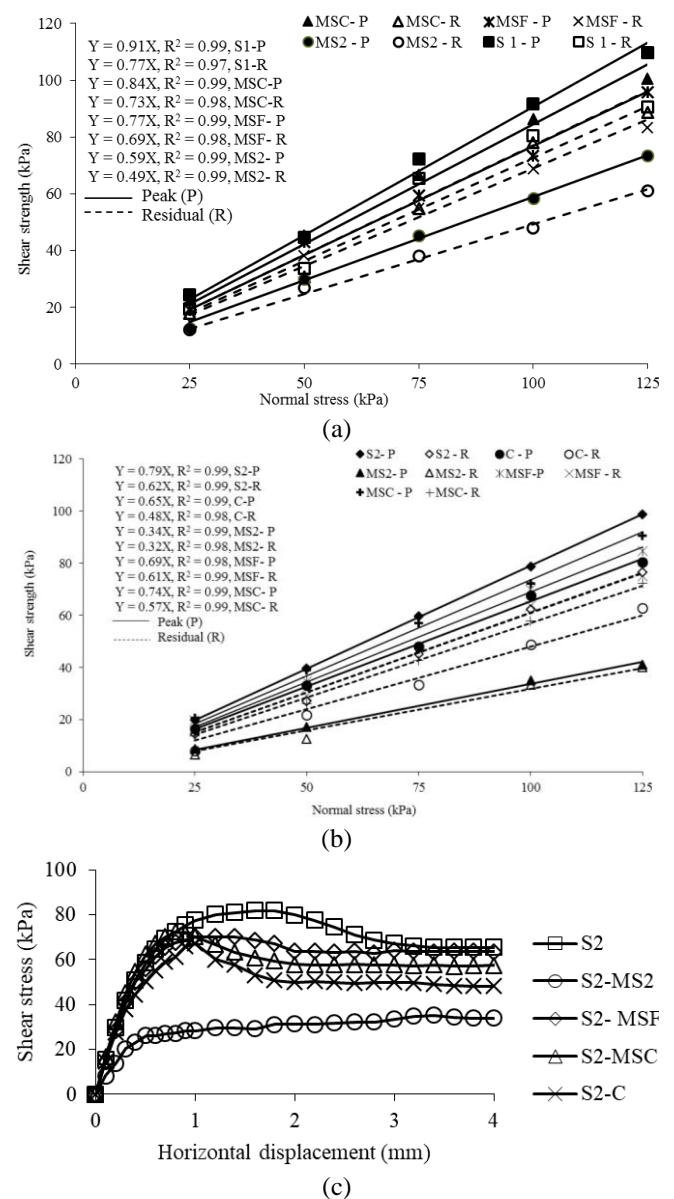

(a)

(b)

(c)

Fig. 5(a) shear strength vs. normal stress envelopes for S1 with different interfaces, (b) shear strength vs. normal stress envelopes for S2 with different interfaces and (c) shear stress vs. horizontal displacement curves for S2 with different interfaces at 100 kPa normal stress

weight of sand, maintaining a constant relative density. Constant normal stress was applied after completely filling the direct shear box and shearing of the sand against different interfaces was performed at a fixed rate of 1.25 mm/min. All the tests were conducted in the normal stress range of 25-125 kPa.

5. Results and discussion

5.1 Effect of surface roughness and mean particle size of sand

Figs. 5(a) and 5(b) show the peak and residual shear strength vs. normal stress relationship of S1 and S2 with different type of interfaces at a relative density of 80%. For the range of normal stresses used in the present study, the peak (P) and residual (R) shear strength profile show a linear trend for both the sands. The solid line in the figure represents the peak shear strength profile while the dashed line shows the residual shear strength profile. Fig. 5(c) shows the shear stress vs. horizontal displacement curves for sand (S2) only and the different type of sand-construction material interfaces at 100 kPa normal stress and 80% relative density. It is clear that for sand only as well as different sand-construction material interfaces, the shear stress vs. horizontal displacement curves show an initial linear portion followed by a nonlinear portion till peak. The shear stress decreases in magnitude after the peak and becomes constant thereafter. This strain softening behavior results in lower residual friction angle than peak friction angle. However, for S2-MS2 interface, the shear stress increases with an increase in horizontal displacement up to the peak value and becomes constant thereafter. This elastoplastic behavior results in nearly identical peak and residual interface friction angles. This indicates that different shearing mechanism exists for S2-MS2 interface (with low surface roughness) and the other interfaces, as discussed later in the section.

Figs. 6(a)-6(d) show the variation of interface friction angle (δ) with surface roughness for S1 and S2. The roughness values for different interfaces were calculated using the similar procedure as described by Subba Rao *et al.* (1998) and Uesugi and Kishida (1986). In the figures, the variation of interfacial friction angle with surface roughness can be divided into two zones. The interface friction angle (peak and residual) increases rapidly with an increase in the roughness of the surface till a particular value (first zone), beyond which there is an insignificant increase in the interface friction angle for both the sands (second zone). The roughness value beyond which the interface friction angles show an insignificant increase is defined as the critical roughness in the present study. Yoshimi and Kishida (1981) reported the interface friction angle of sand-smooth steel interfaces to be as low as 14°. In the present study, interfacial friction angle of 14.5° is observed for smooth interface (MS1) having a ratio of peak and residual interface friction angle to the peak and residual internal friction angle of sand in the range of 0.38-0.4. The residual friction angle is significantly influenced by the surface roughness. For smooth interfaces (MS1), the peak and residual interface friction angles remain nearly
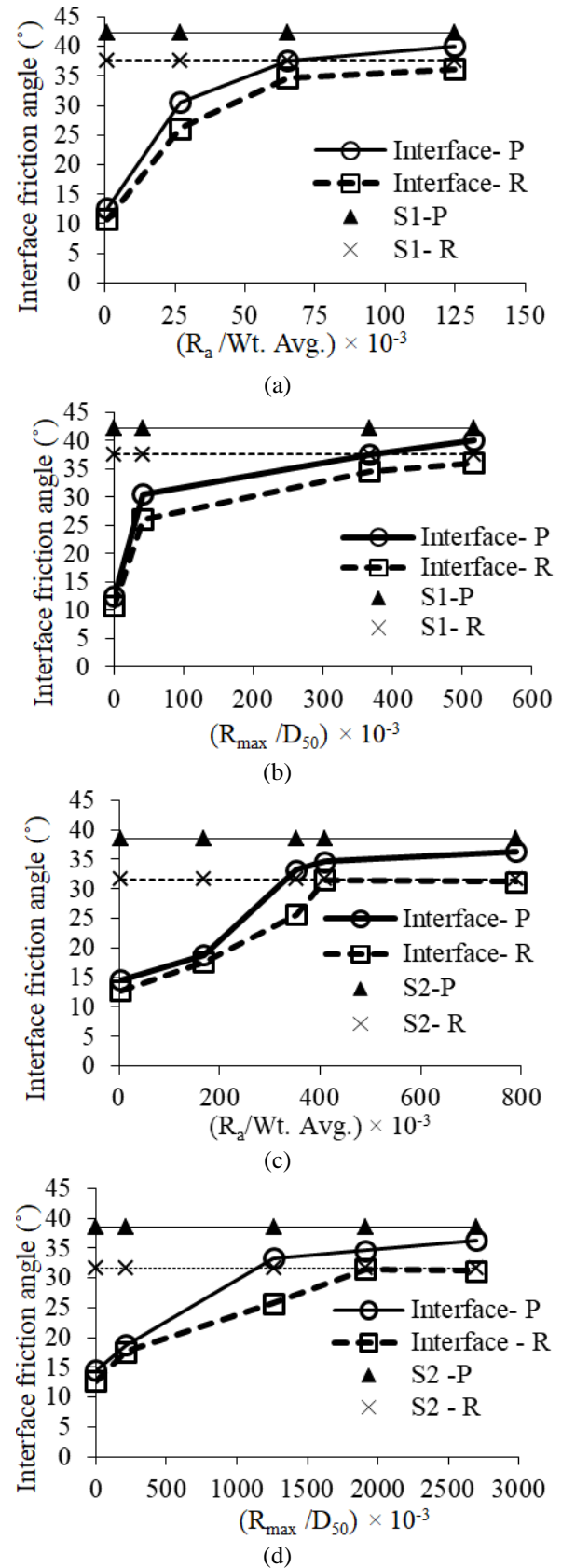

(a)

(b)

(c)

(d)

Fig. 6 Variation of interface frictional angle with surface roughness values for (a) S1 computed similar to Subba Rao *et al.* (1998), (b) S1 computed similar to Uesugi and Kishida (1986), (c) S2 computed similar to Subba Rao *et al.* (1998) and (d) S2 computed similar to Uesugi and Kishida (1986)
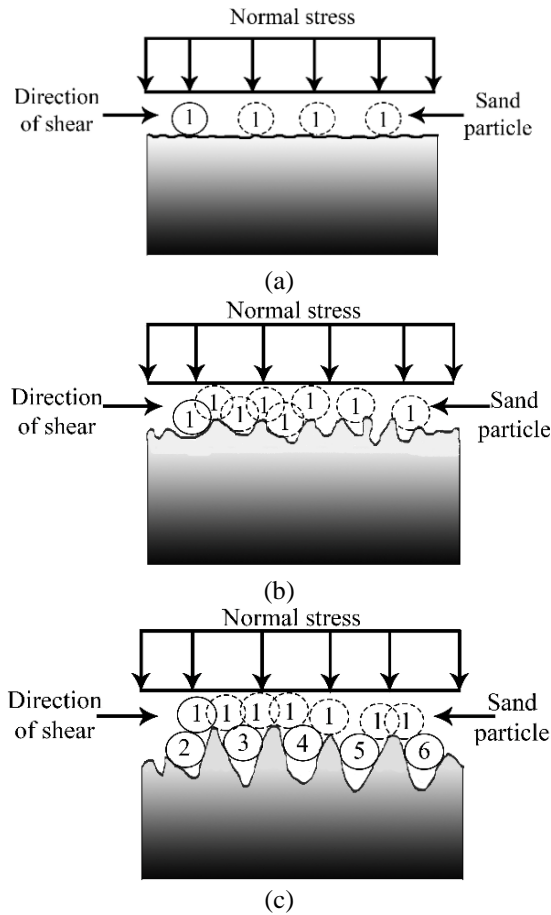
Fig. 7 Mechanism of mobilization of interface shear strength (a) sliding only, (b) sliding and interlocking of sand particles and (c) interlocking and sand-sand friction

The surface roughness of a material is a measure of the size of the asperities present in the surface. For surfaces having low roughness values (i.e., surface with small sized asperities), mobilization of friction between sand and the interface material is the governing shearing mechanism. However, with an increase in the size of asperities in the surface, the roughness value increases. The interlocking of the sand particles with these asperities leads to an increment in the interface friction angle. At critical roughness, all the asperities get filled up with the sand particles and the mobilization of friction begins partly within the sand (adjacent to the interface) and partly on the sand-material (concrete/steel) interface as shown in Fig. 7. In the figure, the position of particles prior to and during shearing is represented by solid and dashed particles respectively.

Fig. 7(a) shows the sliding of the sand particle (1) along the surface of the material with a low surface roughness. Fig. 7(b) shows the interlocking and sliding of the sand particle (1) along the asperities of the surface of material (concrete/steel) (material with moderate surface roughness). Whereas, Fig. 7(c) shows the interlocking and filling of the valley region of the surface with sand particles, resulting in nearly sand-sand shearing along the interface (material with high surface roughness). This indicates that the size of asperities and the particle size of sand play an important role in the interface shearing mechanism. Mobilization of friction is predominant when the surface roughness is very low as compared to the mean particle size of sand (resulting in sliding and rolling of the particles over the surface during shear). The interlocking and sand-sand shearing are predominant when the surface roughness is much larger than the mean particle size of sand. Interlocking and mobilization of friction along the interface is the governing shearing mechanism for the particle size and roughness combinations other than the previously mentioned two extreme cases. Due to the mobilization of the sand friction at critical roughness, the interface friction angle is close to the internal friction angle of sand and the ratio of the two lies in the range of 0.89-0.93. A slight increase in this ratio is observed with further increase in the surface roughness.

Critical roughness values of the interface also depend on the size of sand particles. The mean particle size of S1 and S2 are 1.2 mm and 0.23 mm respectively. Due to the different mean particle size, the critical roughness value is different for the two sands. It must be noted that the method of computing surface roughness does not influence the variation of interface friction angle as the different methods of computing the surface roughness (R_{max} /D_{50} and R_a /Wt. Avg) show similar trend of interface friction angle (Fig. 6).

identical. With an increase in the roughness value, the difference between the peak and residual interface friction angle increases. In the present study, a maximum of 5°-7° difference is observed in the peak and residual interface friction angles. This indicates a change in shear failure mechanism at the interface with an increase in the surface roughness, as discussed later in this section. Chen *et al.* (2015) made a similar observation for the laboratory tests involving red clay and concrete surfaces with different surface roughness.

The critical roughness measured using the similar procedure as described by Subba Rao *et al.* (1998) and Uesugi and Kishida (1986) are 65, 367 and 410, 1913 for S1 and S2 respectively. The ratio of peak and residual interface friction angle to the corresponding peak and residual friction angle of sand at critical roughness is 0.89-0.92 and 0.9-0.93 for sand S1 and S2 respectively. Potyondy (1961), Yoshimi and Kishida (1981), and Acar *et al.* (1982) reported that the limiting interfacial friction angle is equal to the internal friction angle of the medium. In the present study, about 85-92% of the limiting interface shear strength is mobilized at critical roughness values. With an increase in the surface roughness values beyond critical roughness, the peak and residual interface friction angles nearly reach the peak and residual internal friction angle of the medium (sand in the present case).

5.2 Coefficient of friction

Fig. 8 shows the variation of the coefficient of friction at the peak and residual stage over a normal stress range of 25-125 kPa for different interfaces involving S2. The coefficient of friction is expressed as the ratio of shear stress to the normal stress. For all the interfaces, the coefficient of friction corresponding to peak decreases with an increase in the normal stress. Solid lines in the figure represent the coefficient of friction at the peak, while dashed lines represent the coefficient of friction at the residual stage. For the different interfaces used in the
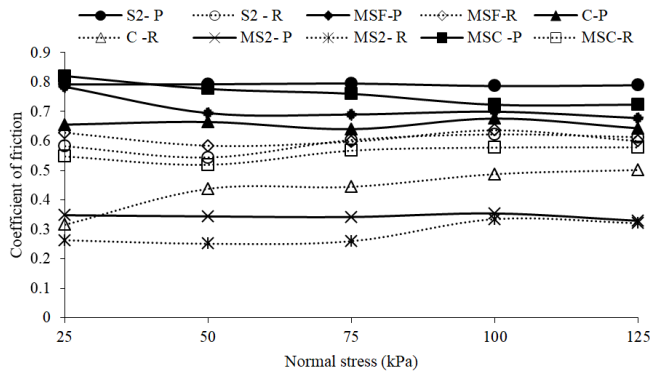
Fig. 8 Variation of coefficient of friction with normal stress for different interfaces

Table 5 Interface friction angle for S2 tested on two different direct shear box

Size of direct shear box = 60 mm×60 mm×25 mm						
Interface	Peak	Ratio	c_{ip}	Residual	Ratio	c_{ir}
S2	38.3	-	-	31.8	-	-
S2–MS1	14.5	0.38	0.33	12.7	0.40	0.36
S2–MS2	18.8	0.49	0.43	17.8	0.56	0.52
S2–C	33	0.86	0.82	25.7	0.81	0.78
S2–MSF	34.6	0.90	0.87	29.7	0.93	0.92
S2–MSC	36.5	0.95	0.94	30	0.94	0.93
Size of direct shear box = 300 mm×300 mm×125 mm						
Interface	Peak	Ratio	c_{ip}	Residual	Ratio	c_{ir}
S2	36	-	-	30	-	-
S2–MS2	15	0.42	0.37	13	0.43	0.40
S2–MSF	28	0.78	0.73	25	0.84	0.81
S2–MSC	34	0.94	0.93	32	1.06	1.08

present study, the coefficient of friction lies in the range of 0.33-0.83 at the peak, while it varies in the range of 0.26-0.63 at the residual stage. Both the peak and residual coefficient of friction increases with an increase in the roughness of the interfaces, due to mobilization of higher interface shear strength (Potyondy 1961, Dove and Frost 1999, Chu and Yin 2005, 2006). MSC (with maximum surface roughness) shows the peak and residual coefficient of friction of 0.74 and 0.57, while MS2 shows a peak and residual coefficient of friction of 0.34 and 0.32 respectively.

5.3 Effect of size of direct shear box

The effect of the size of direct shear box on the interface friction behavior of different interface materials with sand S2 has been investigated using two shear boxes, having dimensions of 60 mm×60 mm×25 mm and 300 mm×300 mm×125 mm. The width to maximum particle size ratio for small and large direct shear boxes is 150 and 750 respectively (for sand S2) and the corresponding ratio of the initial specimen thickness to the maximum particle size is 30 and 156 respectively. Thus, both the direct shear boxes meet the minimum size requirements as per ASTM D3080.

Jewell and Wroth (1987) indicated that the ratio of the length (or width) of the direct shear box to the mean particle size can be used as a measure to scale the direct shear box. The ratio greater than 50 indicates that the test specimens possess sufficient particles to form local rupture and discontinuities, and limits the influence of shear box boundaries on the strength-deformation response. Wu *et al.* (2008) conducted direct shear test on the sand sample using four different square direct shear boxes of size ranging between 40 mm and 800 mm. The internal friction angle was 2°-3° lower for 800 mm direct shear box as compared to 40 mm direct shear box due to the mechanical restraint provided by the shear box.

To compare the results of different interfaces, the interaction coefficient is used along with the ratio of interface friction angle to the corresponding internal friction angle of sand (termed as 'Ratio'). The interaction coefficient (or interface efficiency) is defined as the ratio of shear strength of the interface to the shear strength of soil (Tatlisoz *et al.* 1998, Abu-Farsakh *et al.* 2007).

$$c_i = \frac{c_a + \sigma_n \tan \delta}{c + \sigma_n \tan \varphi} \qquad (1)$$

where c_i=interaction coefficient, c_a=adhesion intercept, c=cohesion intercept, σ_n=normal stress, δ=interface friction angle and φ=angle of internal friction of soil. For the present case (i.e., for sand), the interaction coefficient 'c_i' is reduced to

$$c_i = \frac{\tan \delta}{\tan \varphi} \qquad (2)$$

The interaction coefficient corresponding to peak and residual stage is denoted by c_{ip} and c_{ir} respectively. Table 5 shows the friction angles of different interfaces tested in two different direct shear boxes. It can be observed that both the peak and residual interface friction angles are slightly lower for the tests involving large size direct shear box (300 mm×300 mm×125 mm) as compared to the smaller box. However, the peak as well as residual interaction coefficients for a particular interface, are nearly identical for the small and large size direct shear box. It must be noted that the ratio between interface friction angle and angle of internal friction is nearly identical to the corresponding interaction coefficient.

5.4 Effect of relative density

Tables 6 and 7 show the peak and residual interface friction angles of different interface materials with sand S2 and S1 for two different relative densities respectively. The results suggest that the relative density of the sand significantly influences the peak interface friction angle. The interface friction angle of a particular interface increases with an increase in relative density of the sand due to a better interlocking and greater mobilization of interface friction. However, the peak interaction coefficient of a particular interface for both the sands is nearly identical for 50% and 80% relative density.

Table 6 Interface friction angle for S2 tested on two different relative densities

Interface	Peak	Ratio	c_{ip}	Residual	Ratio	c_{ir}
Relative density = 50%						
S2	33.9	-	-	30.9	-	-
S2–MS1	10.5	0.31	0.28	10	0.32	0.29
S2–MS2	16.9	0.50	0.45	16.3	0.53	0.49
S2-C	29.3	0.86	0.84	26	0.84	0.81
S2-MSF	31.8	0.94	0.92	30.7	0.99	0.99
S2-MSC	32.6	0.96	0.95	31.6	1.02	1.03
Relative density = 80%						
S2	38.3	-	-	31.8	-	-
S2–MS1	14.5	0.38	0.33	12.7	0.40	0.36
S2–MS2	18.8	0.49	0.43	17.8	0.56	0.52
S2-C	33	0.86	0.82	25.7	0.81	0.78
S2-MSF	34.6	0.90	0.87	29.7	0.93	0.92
S2-MSC	36.5	0.95	0.94	30	0.94	0.93

Table 7 Interface friction angle for S1 tested on two different relative densities

Interface	Peak	Ratio	c_{ip}	Residual	Ratio	c_{ir}
Relative density = 50%						
S1	41.7	-	-	40.4	-	-
S1 –MS2	29.3	0.70	0.63	28.9	0.72	0.65
S1-C	33.4	0.80	0.74	33	0.82	0.76
S1-MSF	36.9	0.88	0.84	33	0.82	0.76
S1-MSC	38.8	0.93	0.90	35.5	0.88	0.84
Relative density = 80%						
S1	42.3	-	-	37.6	-	-
S1–MS2	30.6	0.72	0.65	26.1	0.69	0.64
S1-C	39.4	0.93	0.90	34.6	0.92	0.90
S1-MSF	37.6	0.89	0.85	34.6	0.92	0.90
S2-MSC	40.1	0.95	0.93	36.1	0.96	0.95

6. Constitutive modeling of the interface

Constitutive modeling of the interface response offers a distinct advantage of minimizing the number of expensive and time-consuming laboratory experiments. The modeling parameters can be determined from a few laboratory tests, which can be used further to extrapolate the laboratory test data. For modeling the interface behavior of sand with different construction materials (concrete/steel), two methods have been discussed in the present study. The first method is referred as 'A' and the second method as 'B'. The method A involves division of the shear stress vs. horizontal displacement curve into three parts namely, pre-peak, peak and post peak zone. For modeling non-linear pre-peak behavior, the hyperbolic stress-displacement relationship given by Kondner (1963) has been used.

$$\tau = \frac{\delta^*}{\frac{1}{K_s} + \frac{\delta^*}{\tau_{ult}}} \tag{3}$$

where τ=shear stress; δ^*=horizontal displacement; K_s=initial slope of shear stress vs. horizontal displacement curve; τ_{ult}=ultimate shear stress. In Eq. (3), K_s and τ_{ult} are the unknown parameters. These parameters are calculated using the experimental data. The hyperbolic model has been used because of its simplicity as well as high accuracy for modeling non-linear behavior. In some cases, the initial slope of the stress-displacement curve depends on the normal stress. To model such behavior, the expression given by Reddy *et al.* (1996) has been used.

$$K_s = K\gamma_w \left(\frac{\sigma_n}{P_a}\right)^N \tag{4}$$

The instantaneous slope of the stress-displacement curve has been estimated using the expression given by Reddy *et al.* (1996).

$$K_t = K\gamma_w \left(\frac{\sigma_n}{P_a}\right)^N \left(1 - R_f\left(\frac{\tau}{\tau_f}\right)\right)^2 \tag{5}$$

where K_t=instantaneous slope of stress-displacement curve; γ_w=unit weight of water; K=modulus number; N=modulus exponent; σ_n=normal stress; P_a=atmospheric pressure; R_f=failure ratio; τ_f=peak shear stress. Among these parameters, K and N are constants and their values are determined using experimental data. The value of N shows the dependency of the initial slope with the normal stress. Smaller the value of N, lesser is the dependency. The failure ratio gives the relationship between peak and ultimate shear stress.

$$R_f = \left(\frac{\tau_f}{\tau_{ult}}\right) \tag{6}$$

For modeling the peak shear strength, the Mohr-Coulomb's failure criterion has been used

$$\tau_f = c_a + \sigma_n \tan\delta \tag{7}$$

where c_a=adhesion intercept; δ=interface friction angle. The post-peak behavior is modeled using the method proposed by Anubhav and Basudhar (2010). This method is based on the determination of the relationship between horizontal displacement and reduction factor (R). The reduction factor is the post-peak reduction in shear stress normalized by shear stress reduction from peak to residual value. Once the relationship between reduction factor and horizontal displacement is established, the post-peak behavior of the interface can be modeled.

$$R = \left(\frac{\tau_f - \tau}{\tau_f - \tau_r}\right) \tag{8}$$

The second method (method B) is based on the Mohr-Coulomb failure criterion including deviatoric hardening or deviatoric softening, proposed by De Gennaro and Frank (2002). This method consists of three parts: elastic
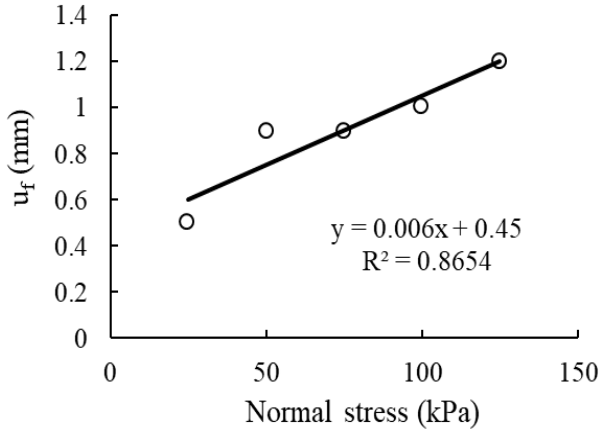
Fig. 9 Variation of u_f with normal stress for S1-C interface at 80% RD of sand

response, yield criterion and plastic response. The plastic response includes strain hardening as well as strain softening behavior. The elastic behavior is modeled using the following set of equations (De Gennaro and Frank 2002, Hu and Pu 2004).

$$d\sigma = K_e du \qquad (9)$$

$$K_e = \begin{bmatrix} K_n & 0 \\ 0 & K_{tan} \end{bmatrix} \qquad (10)$$

$$K_n = k_n \sigma_{ni}^{\ n} \qquad (11)$$

$$K_{tan} = k_t \sigma_{ni}^{\ n} \qquad (12)$$

where K_n and K_{tan} are stiffness of interface in the normal and tangential direction respectively; σ_{ni} is the initial normal stress; the parameters k_n, k_t and n are determined using the experimental data. The failure at the interface is governed by the Mohr-Coulomb's criterion as shown in Eq. (7). For some interfaces, the cohesion can be neglected and the equation can be rewritten as

$$\tau_f = \sigma_n \mu_f \qquad (13)$$

where μ_f=coefficient of friction at failure. For interfaces involving continuous hardening, μ increases continuously with an increase in horizontal displacement, at a decreasing rate, until it becomes equal to μ_f and remains constant thereafter. For modeling this behavior, the expression given by Pietruszczak and Stolle (1987), and De Gennaro and Frank (2002) is used (Eq. (14)).

$$\tau = \left(\mu_0 + \frac{(\mu_f - \mu_0)u_t^p}{A^* \left(\frac{\sigma_{ni}}{p_0}\right) t + u_t^p} \right) \sigma_{ni} \qquad (14)$$

where μ_0=coefficient of friction at the elastic limit; u_t^p=plastic tangential relative displacement; p_0=reference pressure (1 kPa in the present case); A^*=parameter governing shape of stress-displacement curve; t=thickness of shear zone. The thickness of shear zone is assumed to be equal to 10 times the mean particle size of sand (D_{50}) (Pietruszczak and Stolle 1987). The term (σ_{ni}/p_0) shows the effect of initial normal stress on the interface behavior.

For interfaces involving strain softening, the coefficient of friction (μ) increases with an increase in horizontal displacement until it becomes equal to μ_f. After reaching the peak value, it reduces with further increase in horizontal displacement until it becomes equal to the coefficient of friction at residual stage (μ_r). The initial hardening can be modeled using the Eq. (14) and the strain softening zone can be modeled using the Eq. (15) (De Gennaro and Frank 2002).

$$\tau = \left(\mu_r + (\mu_f - \mu_r)\text{sech}\left\{ \frac{A_0}{t}\left(u_t^p - u_{tf}^p\right)\right\} \right)\sigma_{ni} \qquad (15)$$

where A_0 is the parameter governing the shape of the softening regime and u_{tf}^p is the plastic tangential relative displacement corresponding to the peak shear stress. The Eq. (15) is valid only for $u_t^p > u_{tf}^p$. Thus, in the method B, 11 parameters are required (k_t, n, μ_f, μ_0, p_0, A^*, t, μ_r, u_f, u_{tf}^p, A_0). The parameters k_t and n are determined from the initial slope of shear stress vs. horizontal displacement curve at a particular normal stress. As it is very difficult to determine the initial slope exactly, therefore the slope corresponding to u_{t0} is regarded as the initial stiffness. In other words

$$K_{tan} = \left(\frac{\tau}{u_t}\right) at \ u_t = u_{t0} \qquad (16)$$

where $u_{t0}=u_f/2$; u_t=tangential displacement; u_f=displacement corresponding to peak shear stress. For some interfaces, the displacement corresponding to peak shear stress varies with the normal stress. Therefore, a best-fit linear curve is used to predict the value of u_f for a particular value of normal stress (Fig. 9). Thus, the modeling parameters, k_t and n are determined using Eq. (17).

$$k_t = \frac{K_{tan}}{\sigma_{ni}^{\ n}} \qquad (17)$$

The parameters μ_f and μ_r are determined using the experimental data. The parameter μ_0 delimits the elastic zone. Its value corresponds to the coefficient of friction at u_{tf}^e. Here, u_{tf}^e is the elastic tangential relative displacement.

$$u_{tf}^e = \frac{\tau_f}{K_{tan}} \qquad (18)$$

The parameter u_{tf}^p is the plastic tangential relative displacement at failure (corresponding to peak shear stress).

$$u_{tf}^p = u_f - u_{tf}^e \qquad (19)$$

The parameters p_0 and t are reference pressure and thickness of shear zone respectively. p_0 is used to make the
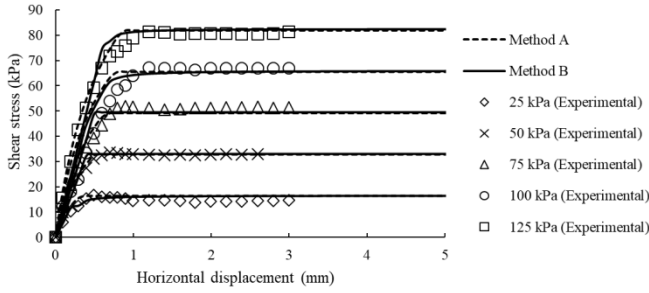
Fig. 10 Experimental vs. predicted stress displacement curves for S1-C at 50% RD of sand
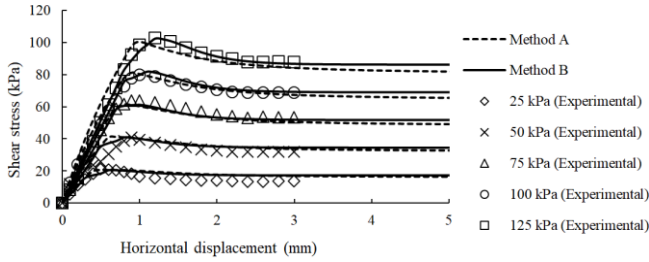

Fig. 11 Experimental vs. predicted stress displacement curves for S1-C at 80% RD of sand

Table 8 Different parameters for Method A

Parameters	R_f	N	K	μ_f	μ_r	a	b	d
S1-C, 50% RD	0.62	0.56	17234	0.66	0.66	-	-	-
S1-C, 80% RD	0.32	0.52	13277	0.82	0.69	1.264	2.1	2.316

Table 9 Different parameters for Method B

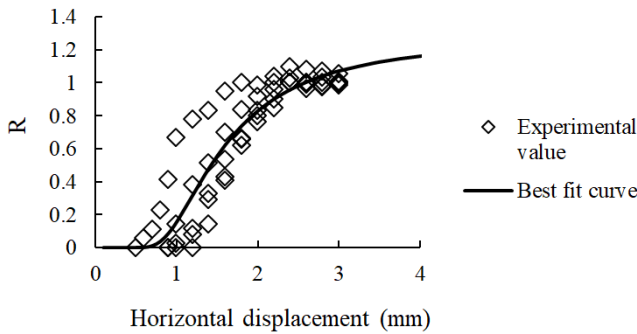| Parameters	k_t (m^{-1})	μ_f	μ_r	A_0	n	t (mm)
S1-C, 50% RD	12880	0.66	0.66	-	0.47	12
S1-C, 80% RD	13684	0.82	0.69	30	0.42	12

Fig. 12 Normalized degradation of shear stress with horizontal displacement for S1-C interface at 80% RD of sand

term (σ_{ni}/p_0) dimensionless. The parameter A^* can be determined by differentiating Eq. (14) with respect to u_t^p and equating it to the initial stiffness at $u_t^p = 0$. Similarly, parameter A_0 is determined using the optimization technique.

6.1 Predicted vs. experimental results

Figs. 10 and 11 show the predicted vs. experimental

stress-displacement curves for the sand-concrete interface (S1-C) at 50% and 80% relative density respectively. It can be observed that the predicted results matched the pre-peak, peak and post peak response of the interface quite well with the experimental results for both the methods. For modeling using method A, 5 parameters (R_f, N, K, μ_f, μ_r) are required along with a relationship between the reduction factor and horizontal displacement. The values of these parameters are derived using the experimental data. The relationship between the reduction factor and horizontal displacement is evaluated using a non-linear regression analysis of the experimental data in MATLAB. Fig. 12 shows the relationship between reduction factor and the horizontal displacement. It can be observed that the relationship follows an S-curve similar to the curve obtained by Anubhav and Basudhar (2010). Eq. (20) shows the equation for the S-curve.

$$y = ae^{-bx^{-d}} \tag{20}$$

The typical values of the parameters used in the two methods are given in Tables 8 and 9 for S1-C interface at 50% and 80% relative densities.

The basic advantage of constitutive modeling is that it can be employed to interpolate the stress-displacement relationship for the interface involving sand and other construction materials, for any normal stress within the tested range of normal stresses.

7. Conclusions

The present paper discusses the role of surface roughness on the interface shear behavior of construction materials (steel and concrete) with sand. Two sands with identical morphological properties and different physical properties have been used to nullify the effect of morphology on the frictional properties. The interfaces with different surface roughness were prepared and tested using a direct shear box. Effect of different parameters including size of direct shear box and relative density of sand medium on the interface behavior have also been evaluated. Finally, constitutive modeling has been conducted and the predicted results are compared with the experimental results. The following conclusions may be drawn from the present study:

• Surface roughness significantly influences the shear response of the interfaces involving sand and concrete/steel. Both the peak and residual interface friction angles increase with an increase in the roughness of the construction material. There exists a critical value of roughness beyond which the increase in the interface friction angle with an increase in surface roughness becomes insignificant.

• The difference between the peak and residual interface friction angle increases with an increase in the surface roughness. For the smooth surface, peak and residual interface friction angles are nearly identical while a difference of 5°-7° is observed for interfaces with high roughness values.

• The ratio of the interface friction angle to the friction angle of sand at critical roughness value for both the sands

used in the present study are in the range of 0.89-0.93. This indicates that nearly 90% of the shear strength of sand is mobilized at critical roughness of the interfaces.

• The variation of interface friction angle with normalized surface roughness computed using different methods viz. relation to the mean particle size, weighted average of different sized particles and the relative height of surface trough over a particular gauge length, is nearly similar. Therefore, the method of computing surface roughness does not influence the interface response.

• Mean grain size of the sand particles influences the critical value of surface roughness for the interface material. In the present study, two morphologically identical sands with different mean particle size showed different value of critical roughness.

• Size of the direct shear box influences the interface friction angle to some extent. Direct shear box having larger size shows a lower value of interface friction angle as compared to small sized box. However, the peak as well as residual interaction coefficients for different interfaces remained nearly identical for the two different sized direct shear boxes used in the present study.

• The relative density of sand significantly influences the peak friction angle of different interfaces. An increase in the interface friction angle is observed with an increase in the relative density of sand. However, the peak interaction coefficient of an interface is nearly identical for 50% and 80% relative density of sand.

• The constitutive model plays a significant role to predict the stress-displacement relationship of the interfaces. The predicted stress-displacement relationship from both the methods matches quite well with the experimental results.

Acknowledgments

References

Abu-Farsakh, M., Coronel, J. and Tao, M. (2007), "Effect of soil moisture content and dry density on cohesive soil-geosynthetic interactions using large direct shear tests", *J. Mater. Civ. Eng.*, **19**(7), 540-549.

Acar, Y.B., Durgunoglu, H.T. and Tumay, M.T. (1982), "Interface properties of sand", *J. Geotech. Geoenviron. Eng.*, **108**(GT4).

Aksoy, H.S., Gor, M. and Inal, E. (2016), "A new design chart for estimating friction angle between soil and pile materials", *Geomech. Eng.*, **10**(3), 315-324.

ASTM D 3080 (2011), *Standard Test Method for Direct Shear Test of Soils Under Consolidated Drained Conditions*, ASTM international, West Conshohocken, Pennsylvania, U.S.A.

Aubry, D., Modaressi, A. and Modaressi, H. (1990), "A constitutive model for cyclic behaviour of interfaces with variable dilatancy", *Comput. Geotech.*, **9**(1-2), 47-58.

Basudhar, P.K. (2010), "Modeling of soil-woven geotextile interface behavior from direct shear test results", *Geotext.*

Geomembr., **28**(4), 403-408.

Boulon, M. and Nova, R. (1990), "Modelling of soil-structure interface behaviour a comparison between elastoplastic and rate type laws", *Comput. Geotech.*, **9**(1-2), 21-46.

Butterfield, R. and Andrawes, K.Z. (1972), "On the angles of friction between sand and plane surfaces", *J. Terramech.*, **8**(4), 15-23.

Cabalar, A.F. (2016), "Cyclic behavior of various sands and structural materials interfaces", *Geomech. Eng.*, **10**(1), 1-19.

Cerato, A. and Lutenegger, A. (2006), "Specimen size and scale effects of direct shear box tests of sands", *Geotech. Test. J.*, **29**(6), 507-516.

Chen, X., Zhang, J., Xiao, Y. and Li, J. (2015), "Effect of roughness on shear behavior of red clay-concrete interface in large-scale direct shear tests", *Can. Geotech. J.*, **52**(8), 1122-1135.

Chu, L.M. and Yin, J.H. (2005), "Comparison of interface shear strength of soil nails measured by both direct shear box tests and pullout tests", *J. Geotech. Geoenviron. Eng.*, **131**(9), 1097-1107.

Chu, L.M. and Yin, J.H. (2006), "Study on soil-cement grout interface shear strength of soil nailing by direct shear box testing method", *Geomech. Geoeng.*, **1**(4), 259-273.

De Gennaro, V. and Frank, R. (2002), "Elasto-plastic analysis of the interface behavior between granular media and structure", *Comput. Geotech.*, **29**(7), 547-572.

Desai, C.S. and Ma, Y. (1992), "Modelling of joints and interfaces using the disturbed-state concept", *J. Numer. Anal. Meth. Geomech.*, **16**(9), 623-653.

Desai, C.S., Zaman, M.M., Lightner, J.G. and Sirirwardane, H.J. (1984), "Thin-layer element for interfaces joints", *J. Numer. Anal. Meth. Geomech.*, **8**(1), 19-43.

Dove, J.E. and Frost, J.D. (1999), "Peak friction behavior of smooth geomembrane-particle interfaces", *J. Geotech. Geoenviron. Eng.*, **125**(7), 544-555.

Dove, J.E. and Jarrett, J.B. (2002), "Behavior of dilative sand interfaces in a geotribology framework", *J. Geotech. Geoenviron. Eng.*, **128**(1), 25-37.

Duncan, J.M. and Clough, G.W. (1971), "Finite element analyses of Port Allen lock", *J. Soil Mech. Found. Div.*, **97**(8), 1053-1068.

FHWA (Federal Highway Administration) (2003), *Geotechnical Engineering Circular No. 7: Soil Nail Walls-Reference Manual*, FHWA Report No. FHWA-NHI-14-007, Washington, D.C., U.S.A.

Frost, J.D., DeJong, J.T. and Recalde, M. (2002), "Shear failure behavior of granular-continuum interfaces", *Eng. Fract. Mech.*, **69**(17), 2029-2048.

Gireesha, N.T. and Muthukkumaran, K. (2011), "Study on soil structure interface strength property", *J. Earth Sci. Eng.*, **4**(6), 89-93.

Goodman, R.E., Taylor, R.L. and Brekke, T.L. (1968), "A model for the mechanics of jointed rocks", *J. Soil Mech. Found. Div.*, **94**(3), 637-659.

Hu, L. and Pu, J. (2004), "Testing and modeling of soil-structure interface", *J. Geotech. Geoenviron. Eng.*, **130**(8), 851-860.

Jewell, R.A. and Wroth, C.P. (1987), "Direct shear tests on reinforced sand", *Geotechnique*, **37**(1), 53-68.

Kishida, H. and Uesugi, M. (1987), "Tests of the interface between sand and steel in the simple shear apparatus", *Geotechnique*, **37**(1), 45-52.

Kondner, R.L. (1963), "Hyperbolic stress-strain response: cohesive soils", *J. Soil Mech. Found. Div.*, **89**(1), 115-144.

Liu, H., Song, E. and Ling, I.H. (2006), "Constitutive modelling of soil structures interface through the concept of critical state soil mechanics", *Mech. Res. Commun.*, **33**(4), 515-531.

Pietruszczak, S. and Stolle, D.F.E. (1987), "Deformation of strain

softening materials Part II: Modelling of strain softening response", *Comput. Geotech.*, **4**(2), 109-123.

Potyondy, J.G. (1961), "Skin friction between various soil and construction material", *Geotechnique*, **11**(4), 393-353.

Punetha, P. and Samanta, M. (2017), "Study on deformed microstructure of geosynthetics in interface direct shear test", *Proceedings of the 6th Indian Young Geotechnical Engineers Conference*, Trichy, India, March.

Punetha, P., Mohanty, P. and Samanta, M. (2016), "Study on interface shear strength of soil-geosynthetics in large direct shear box", *Proceedings of the 6th Asian Regional Conference on Geosynthetics-Geosynthetics for Infrastructure Development,* New Delhi, India, November.

Punetha, P., Mohanty, P. and Samanta, M. (2017), "Microstructural investigation on mechanical behavior of soil-geosynthetic interface in direct shear test", *Geotext. Geomembr.*, **45**(3), 197-210.

Reddy, E.S., Chapman, D.N. and Sastry, V.V.R.N. (2000), "Direct shear interface test for shaft capacity of piles in sand", *Geotech. Test. J.*, **23**(2), 199-205.

Reddy, K.R., Kosgi, S. and Motan, E.S. (1996), "Interface shear behavior of landfill composite liner systems: A finite element analysis", *Geosynth.*, **3**(2), 247-275.

Shahrour, I. and Rezaie, F. (1997), "An elastoplastic constitutive relation for the soil-structure interface under cyclic loading", *Comput. Geotech.*, **21**(1), 21-39.

Sharma, M., Samanta, M. and Sarkar, S. (2016), "A study on comparison of pullout behavior of helical and conventional driven soil nails", *Proceedings of the International Geotechnical Engineering Conference on Sustainability in Geotechnical Engineering Practices and Related Urban Issues*, Mumbai, India.

Sharma, M., Samanta, M. and Sarkar, S. (2017), "A laboratory study on pullout capacity of helical soil nail in cohesionless soil", *Can. Geotech. J.*, **54**(10), 1482-1495.

Subba Rao, K.S., Allam, M.M. and Robinson, R.G. (1998), "Interfacial friction between sands and solid surfaces", *Proc. Inst. Civ. Eng. Geotech. Eng.*, **131**(2), 75-82.

Tatlisoz, N., Edil, T.B. and Benson, C.H. (1998), "Interaction between reinforcing geosynthetics and soil-tire chip mixtures", *J. Geotech. Geoenviron. Eng.*, **124**(11), 1109-1119.

Tejchman, J. and Wu, W. (1995), "Experimental and numerical study of sand-steel interfaces", *J. Numer. Anal. Meth. Geomech.*, **19**(8), 513-536.

Toufigh, V., Shirkhorshidi, S.M. and Hosseinali, M. (2017), "Experimental investigation and constitutive modeling of polymer concrete and sand interface", *J. Geomech.*, **17**(1), 04016043.

Tsubakihara, Y. and Kishida, H. (1993), "Frictional behaviour between normally consolidated clay and steel by two direct shear type apparatuses", *Soil. Found.*, **33**(2), 1-13.

Uesugi, M. and Kishida, H. (1986), "Influential factors of friction between steel and dry sands", *Soil. Found.*, **26**(2), 33-46.

Vangla, P. and Latha, G.M. (2016), "Effect of particle size of sand and surface asperities of reinforcement on their interface shear behavior", *Geotextiles and Geomembranes*, **44**(3), 254-268.

Vieira, C.S., Lopes, M.D.L. and Caldeira, L. (2015), "Sand-Nonwoven geotextile interfaces shear strength by direct shear and simple shear tests", *Geomech. Eng.*, **9**(5), 601-618.

Wu, W., Wick, H., Ferstl, F. and Aschauer, F. (2008), "A tilt table device for testing geosynthetic interfaces in centrifuge", *Geotext. Geomembr.*, **26**(1), 31-38.

Yoshimi, Y. and Kishida, T. (1981), "A ring torsion approach for evaluating friction between soil and metal surfaces", *Geotech. Test. J.*, **4**(4), 145-152.

Zhang, C., Ji, J., Gui, Y., Kodikara, J., Yang, S.Q. and He, L. (2016), "Evaluation of soil-concrete interface shear strength based on LS-SVM", *Geomech. Eng.*, **11**(3), 361-372.

CC